

# AFFINE INVARIANT SURFACE EVOLUTIONS FOR 3D IMAGE SEGMENTATION

*Yogesh Rathi, Peter Olver, Guillermo Sapiro, Allen Tannenbaum*

## ABSTRACT

In this paper we present an algorithm for 3D medical image segmentation based on an affine invariant flow. The algorithm is simple to implement and semi-automatic. The technique is based on active contours evolving in time according to intrinsic geometric measures of the image. The surface flow is obtained by minimizing a global energy with respect to an affine invariant metric. Affine invariant edge detectors for 3-dimensional objects are also computed which have the same qualitative behavior as the Euclidean edge detectors. This algorithm yields better segmentation results, since the affine symmetry group is much larger than the Euclidean group. Results on artificial and real MRI images show that the algorithm performs well, both in terms of accuracy and robustness to noise.

## 1. INTRODUCTION

This paper is devoted to the analysis and implementation of the motion of a surface in a conformal affine space with application to segmentation of homogeneous regions in 3D images.

Image segmentation is an important step for almost all image analysis. The active contour methodology in the level sets framework [1, 2, 3] has been found to be a powerful tool for extracting objects of interest. In these methods, starting from an initial estimate, the curve deforms under the influence of various forces until it fits the object boundaries. The curve evolution equation is obtained by decreasing an image based energy  $E_{image}$  as fast as possible, i.e., by doing a gradient descent on  $E_{image}$ . In general,  $E_{image}$  may depend on a combination of image based features and external constraints (smoothness, shape etc) [4, 5]. The level set methods of Osher and Sethian [6] offer a natural and numerically robust implementation of such curve evolution equations. Level sets have the advantage of being parame-

ter independent (i.e. they are implicit representation of the curve) and can handle topological changes naturally.

Several active contour models for segmentation [2, 3] in 2D and 3D space have been proposed. Affine invariant gradient snakes have been proposed in [7]. This is part of a program to incorporate invariant detection, segmentation, and denoising schemes in object recognition systems to reduce the algorithmic noise introduced by using non-invariant methods. In this note, we show how the methodology of [7] may be easily extended to the 3D case. Affine invariant flows are particularly attractive since they still only involve two spatial derivatives as for the standard geometric active contour models. They may also have greater numerical stability. Moreover the affine invariant flow is most natural for scale-space given the fact that the group of invariants is much larger, but nevertheless the number of spatial derivatives remains the same as for the Euclidean group. See [8] for the details.

The proposed method addresses this problem by segmenting such 3D images naturally by evolving a surface in  $\mathbf{R}^3$ . We show that 3D objects can be segmented in an affine invariant manner by considering a conformally weighted volume form. The conformal factor must be chosen to be affine invariant. We note that volume is invariant with respect to the (special) affine group, and is a relative invariant with respect to the full affine group.

Because of considerations of space, we will only be able to outline some of our basic ideas. A full invariant system for image processing will be published in a more detailed version of this work.

## 2. BASIC FLOW

In this section we state the fundamental flow for the affine invariant segmentation method. Let  $R$  be an open connected bounded subset of  $\mathbf{R}^n$  (in our case  $\mathbf{R}^3$ ) with smooth boundary  $S = \partial R$ . Let  $\Psi : R \rightarrow \mathbf{R}^n$  be a family of embeddings, such that  $\Psi^0$  is the identity. Let  $\phi : \mathbf{R}^n \rightarrow \mathbf{R}$  be a positive  $C^1$  function. Set  $R(t) = \psi^t(R)$  and  $S(t) = \psi^t(\partial R)$ . Consider the family of  $\phi$ -weighted volumes

$$\begin{aligned} H(t) &= \int_R \phi(\psi^t(\mathbf{x})) d\psi^t(\mathbf{x}) \\ &= \int_{R(t)} \phi(\mathbf{y}) d\mathbf{y} \end{aligned} \tag{1}$$

---

Yogesh Rathi and Allen Tannenbaum are with the Schools of Electrical & Computer and Biomedical Engineering, Georgia Institute of Technology, Atlanta, GA 30332-0250; yogesh.rathi@bme.gatech.edu, tannenba@ece.gatech.edu. Peter Olver is with the Department of Mathematics, University of Minnesota, Minneapolis, MN 55455; olver@math.umn.edu. Guillermo Sapiro is with the Department of Electrical and Computer Engineering, University of Minnesota, Minneapolis, MN 55455; guille@ece.umn.edu. This research was supported by grants from NSF, NIH, AFOSR, ARO, and ONR.

Set  $X = \frac{\partial \psi^t}{\partial t} |_{t=0}$ , then using the area formula [9] and then by the divergence theorem, the first variation is

$$\begin{aligned} \frac{dH}{dt} |_{t=0} &= \int_R \operatorname{div}(\phi X) dx \\ &= - \int_{\partial R} (\phi X) \cdot N dy \end{aligned} \quad (2)$$

where  $N$  is the inward unit normal to  $S = \partial R$ . Consequently the corresponding  $\phi$ -weighted affine invariant volume minimizing flow is

$$\frac{\partial S}{\partial t} = \phi \kappa^{1/4} N, \quad (3)$$

where  $\kappa$  is the Gaussian curvature [11]. This flow is only defined for convex surfaces. As argued in [8], in order to extend this to concave surfaces, one should consider a flow of the form

$$\frac{\partial S}{\partial t} = \phi \kappa_+^{1/4} \operatorname{sign}(H) N \quad (4)$$

where  $\kappa_+ = \max(\kappa, 0)$  and  $\operatorname{sign}(H)$  is the sign of the mean curvature of the surface.

### 3. AFFINE INVARIANT GRADIENT

Let  $I : \mathbf{R}^3 \rightarrow \mathbf{R}^+$  be a given 3D grey scale image. To detect edges in an affine invariant form, a possible approach is to replace the classical gradient magnitude  $\|\nabla I\| = (I_x^2 + I_y^2 + I_z^2)^{1/2}$ , which is only Euclidean invariant, with an affine invariant function from  $\mathbf{R}^3$  to  $\mathbf{R}$  that has, at image edges, values significantly different from those at flat areas and such that these values are preserved, at corresponding image points, under affine transformations. To accomplish this, we have to verify that we can use basic affine invariant descriptors that can be computed from  $I$  in order to find an expression that qualitatively behaves like  $\|\nabla I\|$ . Following [7], we formulate two basic independent affine invariant descriptors in 3D space as

$$\begin{aligned} H &= \det \begin{pmatrix} I_{xx} & I_{xy} & I_{xz} \\ I_{yx} & I_{yy} & I_{yz} \\ I_{zx} & I_{zy} & I_{zz} \end{pmatrix} \\ &= I_{xx}(I_{yy}I_{zz} - I_{zy}^2) - I_{xy}(I_{yx}I_{zz} - I_{yz}I_{zx}) \\ &\quad + I_{xz}(I_{yx}I_{zy} - I_{zx}I_{yy}) \end{aligned} \quad (5)$$

$$\begin{aligned} J &= I_x^2(I_{yy}I_{zz} - I_{zy}^2) + I_y^2(I_{xx}I_{zz} - I_{xz}^2) \\ &\quad + I_z^2(I_{xx}I_{yy} - I_{xy}^2) + 2I_xI_y(I_{xz}I_{yz} - I_{xy}I_{zz}) \\ &\quad + 2I_yI_z(I_{xy}I_{xz} - I_{yz}I_{xx}) + 2I_xI_z(I_{xy}I_{yz} - I_{xz}I_{yy}) \end{aligned} \quad (6)$$

There is no non-trivial first-order affine invariant descriptor, and all other second-order differential invariants are functions of  $H$  and  $J$ . Therefore the simplest possible affine

gradient must be expressible as a function  $F(H, J)$  of these two invariant descriptors.

The differential invariant  $J$  is related to the Euclidean curvature of the level sets of the image. Indeed, if a surface  $S$  is defined as the level set of a 3D image  $I$ , then the Gaussian curvature of  $S$  is given by  $\kappa = (J/\|\nabla I\|^4)$ . Lindeberg [10] used  $J$  to compute corners and edges (for 2D images) in an affine invariant form, that is,

$$F = J = \kappa \|\nabla I\|^4$$

This singles out the image structures with a combination of high gradient(edges) and high curvature of the level sets (corners). Note that, in general, edges and corners do not have to lie on a unique level set. Here, by combining both  $H$  and  $J$ , we present a more general affine gradient approach. Because both  $H$  and  $J$  are second order derivatives of the image, the order of the affine gradient is not increased while both invariants are being used.

We define the basic affine invariant gradient of a function  $I$  by the equation

$$\nabla_{aff} I = \left| \frac{H}{J} \right|$$

Technically, because  $\nabla_{aff} I$  is a scalar, it measures just the magnitude of the affine gradient, so our definition may be slightly misleading. However, an affine invariant gradient direction does not exist, as directions (angles) are not affine invariant, and so we are justified in omitting direction for simplicity.

The justification for our definition is based on a simplified analysis of the behavior of  $\nabla_{aff} I$  near edges in the image defined by  $I$ . Near the edge of an object, the gray-level values of the image can be (ideally) represented by  $I(x, y, z) = f[z - h(x, y)]$ , where  $z = h(x, y)$  is the edge of the surface and  $f(t)$  is a slightly smoothed step function with a jump near  $t = 0$ . Straightforward computations show that, in this case

$$\begin{aligned} H &= f'' f'^2 (h_{xx}h_{yy} - h_{xy}^2) \\ J &= f'^4 (h_{xx}h_{yy} - h_{xy}^2) \end{aligned} \quad (7)$$

Therefore,

$$\frac{H}{J} = \frac{f''}{f'^2} = \left( \frac{-1}{f'} \right)' \quad (8)$$

Clearly,  $H/J$  is large (positive or negative) on either side of the object  $z = f(x, y)$ , creating an approximation of a zero crossing at the edge (Figure 1). (Note that the Euclidean gradient is the opposite, high at the ideal edge and zero elsewhere. Of course, this does not make any fundamental

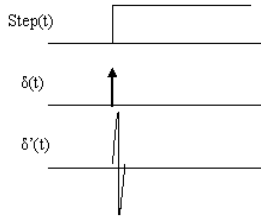


**Fig. 1.** Function  $f(t)$  and its derivatives at the edges.

difference, as the important part is to differentiate between edges and flat regions. In the affine case, edges are given by doublets.) This is because  $f(t) = \text{step}(t)$ ,  $f'(t) = \delta(t)$ , and  $f''(t) = \delta'(t)$ , where we ignore points with  $f' = 0$ . Therefore  $\nabla_{aff} I$  behaves like the classical Euclidean gradient magnitude.

To avoid possible difficulties when the affine invariants  $H$  or  $J$  are zero, we replace  $\nabla_{aff}$  with a slight modification. In Euclidean invariant edge-detection algorithms based on active contours as well as in anisotropic diffusion, the stopping term is usually taken in the form  $(1 + \|\nabla I\|^2)^{-1}$ , the extra 1 being taken to avoid singularities where the gradient vanishes. Thus in analogy, the corresponding affine invariant stopping term should have the form

$$\frac{1}{1 + (\nabla I)^2} = \frac{J^2}{H^2 + J^2}$$

However, this can still present difficulties when both  $H$  and  $J$  vanish, so a second modification is proposed.

The normalized affine invariant gradient is given by

$$\nabla_{aff} I = \left( \frac{H^2}{J^2 + 1} \right)^{1/2} \quad (9)$$

Now the affine invariant stopping term is given by

$$\phi(x, y, z) = \frac{1}{1 + (\nabla_{aff} I)^2} = \frac{J^2 + 1}{H^2 + J^2 + 1} \quad (10)$$

Equation (10) avoids all the difficulties of the previous formulation where  $H$  and  $J$  both vanish. For further details see [11].

#### 4. EXPERIMENTS

2D planar contours used for segmenting a volumetric image (3D) requires segmenting each of the slices in 2D. This method is quite unnatural and time consuming. The proposed surface evolution segmentation algorithm can segment images directly in 3D. Some segmentation results obtained using the proposed method are shown in Figures 2-4.

Note that, the segmentation is the result of a single surface evolution. Since it is difficult to define an initial starting surface which encapsulates the desired object, we define several small spheres within the object of interest and use an inflationary term to expand these spheres out and then use the surface evolution to get at the boundary of the desired object. Since curvature is a diffusive term, simple central differences can be used to evaluate the mean and gaussian curvature terms. For further details on numerical implementation of level set methods, see [12].

#### 5. REFERENCES

- [1] R. Malladi, J. A. Sethian, and B. C. Vemuri, "Shape modeling with front propagation: A level set approach," *IEEE Transactions on Pattern Analysis and Machine Intelligence*, vol. 17, no. 2, pp. 158–175, 1995.
- [2] S. Kichenassamy, A. Kumar, P. Olver, A. Tannenbaum, and A. Yezi, "Conformal curvature flows: From phase transitions to active vision," *Archive for Rational Mechanics and Analysis*, vol. 134, no. 3, pp. 275–301, 1996.
- [3] V. Caselles, R. Kimmel, and G. Sapiro, "Geodesic active contours," *International Journal of Computer Vision*, vol. 22, no. 1, pp. 61–79, 1997.
- [4] D. Mumford and J. Shah, "Optimal approximation by piecewise smooth functions and associated variational problems," *Commun. Pure Applied Mathematics*, vol. 42, pp. 577–685, 1989.
- [5] T. Chan and L. Vese, "Active contours without edges," *IEEE Transactions on Image Processing*, vol. 10, no. 2, pp. 266–277, 2001.
- [6] S. J. Osher and J. A. Sethian, "Fronts propagation with curvature dependent speed: Algorithms based on hamilton-jacobi formulations," *Journal of Computational Physics*, vol. 79, pp. 12–49, 1988.
- [7] G. Sapiro P. Olver and A. Tannenbaum, "Affine invariant edge detection: edge maps, anisotropic diffusion and active contours," *Acta. Math. Appl.*, vol. 59, 1999.
- [8] V. Caselles and C. Sbert, "What is the best causal scale-space for 3d images?," *Technical Report: Dept. of Math. and Comp. Sciences, Univ. of Illes Balears, Spain*, 1994.
- [9] L. Simon, "Lectures on geometric measure theory," in *Proceedings of the Center for Mathematical Analysis, Australian National Univ., Canberra*, 1983.
- [10] T. Lindeberg, "Scale-space theory in computer vision," *Kluwer, Dordrecht, The Netherlands*, pp. 488–492, 1994.
- [11] G. Sapiro, *Geometric Partial Differential Equations and Image Analysis*, Cambridge University Press, 2000.
- [12] J. A. Sethian, *Level Set Methods and Fast Marching Methods*, Cambridge University Press, 2nd edition, 1999.

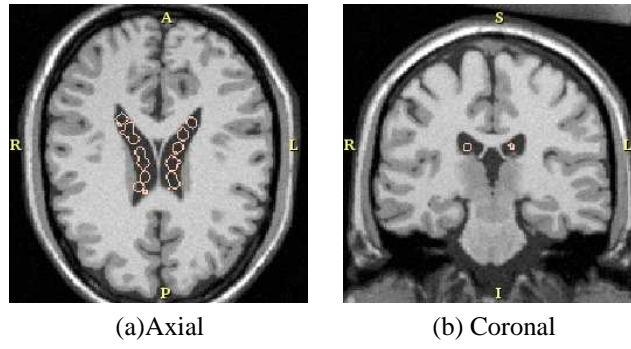


**Fig. 2.** Starting Contour for Axial and Coronal slices

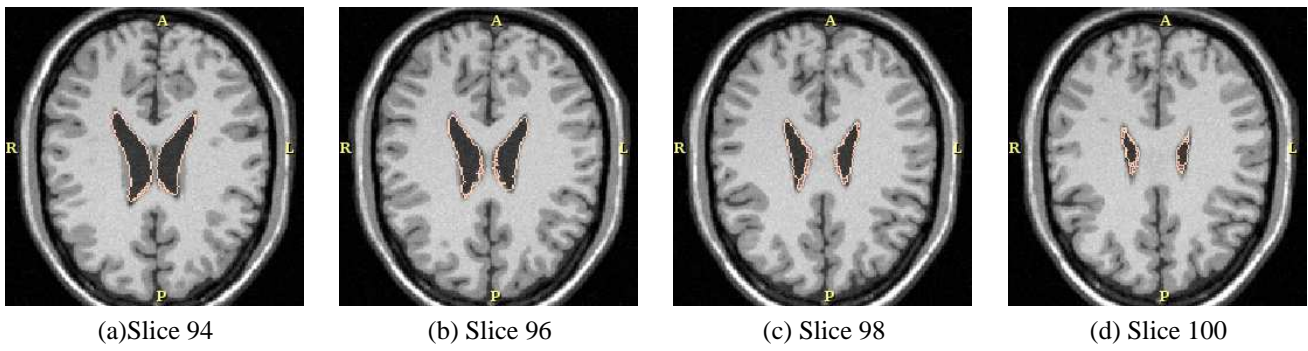


**Fig. 3.** Contour Evolution for various Axial slices

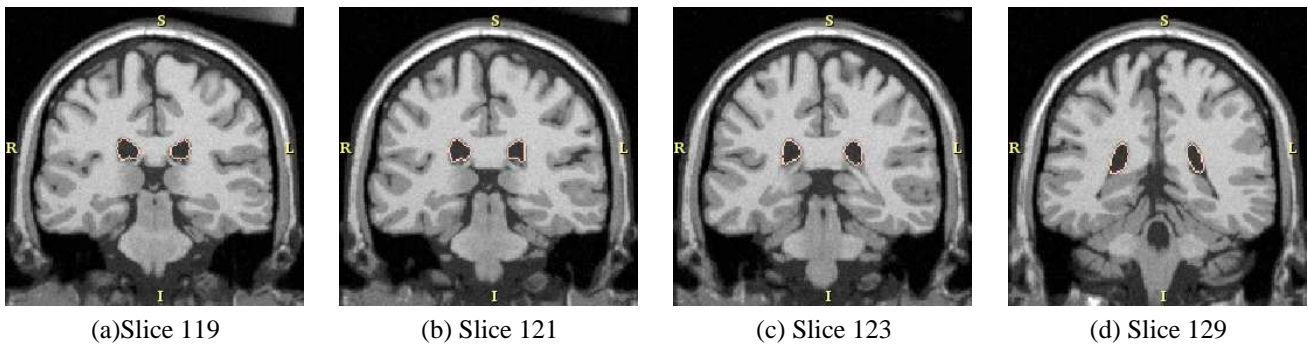


**Fig. 4.** Contour Evolution for various Coronal slices

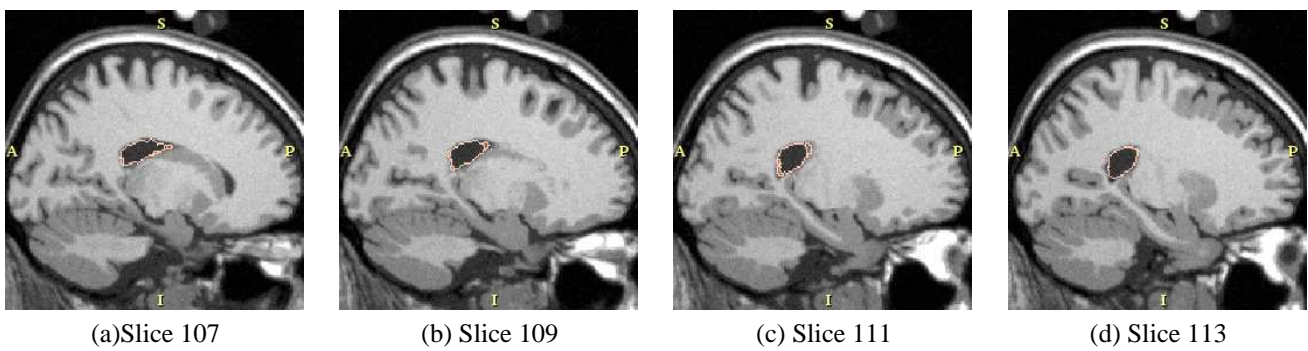


**Fig. 5.** Contour Evolution for various Sagittal slices